ISSN 1029-9599, Physical Mesomechanics, 2022, Vol. 25, No. 4, pp. 318–325. © Pleiades Publishing, Ltd., 2022.
Russian Text © The Author(s), 2022, published in Fizicheskaya Mezomekhanika, 2022, Vol. 25, No. 2, pp. 47–55.

Superplastic Behavior of Fine-Grained Al-Mg-Li Alloy

G. F. Korznikova[1]*, G. R. Khalikova[1,2], S. Yu. Mironov[3], A. F. Aletdinov[1], E. A. Korznikova[2,4], T. N. Konkova[1,5], and M. M. Myshlyaev[6]

[1] *Institute for Metal Superplasticity Problems, Russian Academy of Sciences, Ufa, 450001 Russia*
[2] *Ufa State Petroleum Technological University, Ufa, 450062 Russia*
[3] *Belgorod State University, Belgorod, 308015 Russia*
[4] *Ufa State Aviation Technical University, Ufa, 450000 Russia*
[5] *University of Strathclyde, Glasgow, G1 1XJ United Kingdom*
[6] *Baikov Institute of Metallurgy and Materials Science, Russian Academy of Sciences, Moscow, 119334 Russia*
** e-mail: gfkorznikova@gmail.com*

Received August 12, 2021; revised December 21, 2021; accepted December 27, 2021

Abstract—The superplastic behavior of fine-grained 1420 Al-Mg-Li alloy was investigated using a modern electron microscopy technique based on automatic analysis of electron backscattered diffraction patterns (EBSD analysis). The generally accepted idea that grain boundary sliding is dominant during superplastic flow suggests the preservation of an equiaxed fine-grained structure with predominantly high-angle grain boundary misorientation in the material. The present study revealed that heating prior to the onset of deformation leads to some grain growth due to static recrystallization, and superplastic deformation is accompanied by dynamic grain growth and continuous dynamic recrystallization. Continuous recrystallization has a more significant effect on microstructural changes. This mechanism involves the transverse division of pre-elongated grains into subgrains that ultimately transform into chains of nearly equiaxed small grains, resulting in a bimodal grain structure. The data obtained, including significant strain hardening, noticeable grain elongation, the formation of a well-defined dislocation structure and subboundaries within grains, as well as the development of a pronounced crystallographic texture, provide convincing evidence of the occurrence of intragranular slip during superplastic flow throughout the entire volume of the material. A comprehensive analysis of a wide range of experimental data showed that intragranular slip plays an essential role in superplastic flow, and its contribution can be much larger than previously thought. The results obtained contribute to a better fundamental understanding of the superplasticity phenomenon.

Keywords: superplasticity, aluminum alloys, microstructure, mechanical behavior

DOI: 10.1134/S1029959922040051

1. INTRODUCTION

The phenomenon of superplasticity, identified by C.E. Pearson in 1934, was first of purely scientific interest as an unusual tensile behavior of Sn-based alloys. Later, when it became clear that many metal materials could be brought to superplasticity, great practical interest in the phenomenon aroused. In the last 50 years or thereabouts, the effect of superplasticity has been scrutinized and its conditions and main mechanisms responsible for high elongation without failure have been established. According to the generally accepted concept of superplastic deformation, its basic prerequisite is a rather fine equiaxed structure with a large fraction of high-angle boundaries. It is thought that such a structure is best suited for grain boundary sliding as the key mechanism of superplasticity.

However, recent studies convincingly demonstrate that materials with an "imperfect" microstructure, e.g., with a partially recrystallized microstructure rich in low-angle boundaries, can also display superplasticity. Among such materials can be aluminum alloys [1–6], titanium alloys [7], steels [8], very coarse-grained (~100 μm) materials [9, 10], and even materials with lamellar microstructures [11]. In all of them, the initial stage of superplastic deformation is associated with dynamic recrystallization, which transforms their imperfect microstructure into a typical fine one and normally against pronounced strain hardening; and further steady flow, with activated

grain boundary sliding. In general, these recent data agree with previous theories which put forward a close link between superplasticity and dynamic recrystallization as far back as 1960s–1990s [1–15]. Notwithstanding the significance of the above data, they refer mostly to the macroscale traceable by conventional metallography, transmission electron microscopy, and X-ray methods available at that time. The now available digital method of electron backscatter diffraction (EBSD), which combines the means of metallography and X-ray diffraction analysis, provides large statistical data samples to inquire into a qualitatively new scale—the mesoscale. Although the number of EBSD studies is scanty, such studies are undeniably needed for clarifying the essence of superplasticity. In particular, EBSD data show that materials after superplastic deformation reveal clear evidence of developed intragranular glide even with a perfectly fine recrystallized structure [16–18]. The aim of our study is to analyze the microstructure and superplastic behavior of perfectly fine-grained recrystallized aluminum alloy 1420 (Al-Mg-Li). This material refers to the relatively new generation of aircraft-grade aluminum alloys with a high specific strength, good weldability, and good potential for use in aerospace industry.

2. RESEARCH TECHNIQUE

The test material was aluminum alloy 1420 (Al-5.5Mg-2.2Li-0.12Zr, mass %), whose superplastic behavior is well understood. Initially, it was a hot-rolled bar having a fully recrystallized microstructure with an average grain size of 20 μm. To test the alloy for superplasticity, its microstructure was brought to a fine-grained state by annealing at 470°C for 1 h with water quenching and by further equal-channel angular pressing in ten BC passes through a square route of 90° at 370°C. Then, flat specimens with a gage section of $5 \times 3 \times 0.8$ mm^3 were cut along the longitudinal axis of the material and were mechanically polished to be uniform in thickness and free of surface defects. The temperature of tensile tests was 370°C ($\approx 0.8T_m$, where T_m is the melting point). As has been shown [19], this temperature is optimal for the effect of superplasticity in fine-grained alloy 1420. All tensile tests were performed on an Instron machine at a constant loading rate which corresponded to a nominal strain rate of 3×10^{-2} s^{-1}. Before each experiment, the test specimens were kept at 370°C for 8 min to attain thermal equilibrium, and after the deformation, they were quenched in water. The rate sensitivity m was determined by varying the tensile strain rate between 3×10^{-2} and 6×10^{-2} s^{-1}. For engineering-to-true curve conversion, the volume was assumed to be constant and the strain to be uniform. To compensate the continuous decrease in the true strain rate in tension, the true stress–true strain curves were corrected through multiplying each stress point by $(L/L_0)_m$, where L is the instantaneous length of the gage section, L_0 is its initial length, m is the rate sensitivity.

The microstructure in the specimen gage section was examined on a JEM 2100 Plus transmission electron microscope at an accelerating voltage of 200 kV and on a TESCAN MIRA scanning electron microscope (EBSD analysis) at an accelerating voltage of 20 kV. The software for statistical data analysis, including average grain size measurements, was a CHANNEL 5.0 program package with a confidence probability of 95%. The step size of EBSD maps was 0.2 μm; the maximum orientation error was 2°. To increase the reliability of EBSD data, all fine grains of three pixels and less were automatically "cleared" by standard color codes available in the EBSD software. The maps of crystallographic orientations presented below show them in different color with low-angle ($2° < \Theta < 15°$) and high-angle boundaries ($\Theta \geq 15°$) distinguishable by white and black lines, respectively.

3. RESEARCH RESULTS

3.1. Mechanical Behavior

As can be seen from typical tensile stress–strain curves in Fig. 1, the total elongation for an optimum superplasticity temperature of 370°C at an initial strain rate of 3×10^{-2} s^{-1} measures more than 900% up to fracture (Fig. 1a) and corresponds to a true strain of 2.3 (Fig. 1b). Thus, in phenomenological terms, the fine-grained alloy after equal-channel angular pressing shows the main sign of superplasticity—high elongation before fracture. The true stress–true strain curve (Fig. 1b) is characterized by pronounced hardening, its peak, and further softening during superplastic deformation. Although no clear evidence of steady superplastic flow is found, all true stress–true strain curves of the material are evidently humped and well consistent with its superplastic behavior reported elsewhere [19]. The hardening of the material during its superplastic deformation can be due to active intragranular glide and/or dynamic grain growth, as evidenced by our research data and

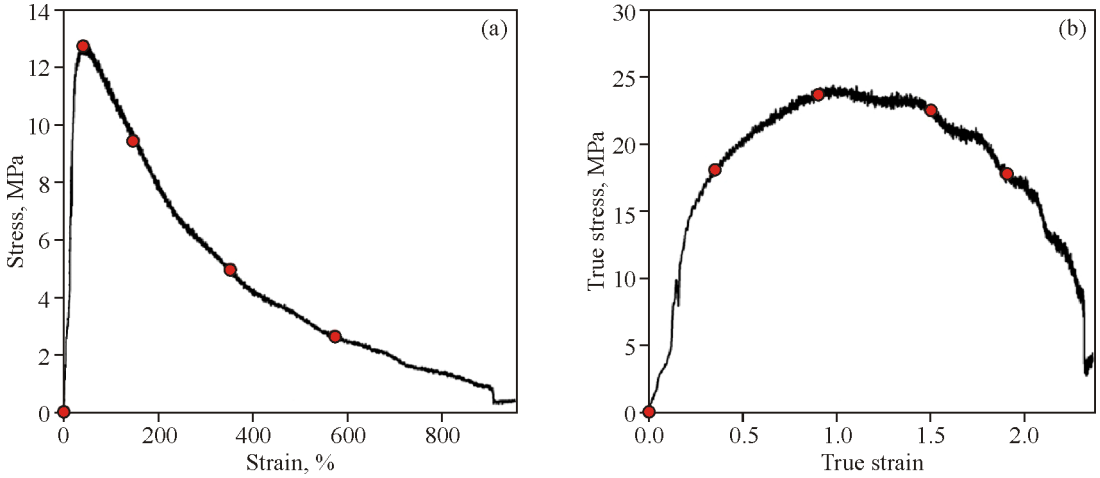

Fig. 1. Engineering (a) and true stress–strain curve (b) for aluminum alloy 1420 under superplastic conditions.

data available from other sources [1, 16–19]. Additionally, the superplastic behavior of the material is confirmed by the strain rate sensitivity measuring $m \sim 0.45$ for flow stresses under the temperature-rate conditions used [18, 20, 21] and approximating $m \sim 0.5$ for ideal superplasticity.

It should be noted that the alloy showed superplasticity at relatively high strain rates because of the very fine grain size in its specimens after equal-channel angular pressing. Such fine-grained materials feature both high-rate and low-temperature superplasticity [22], which is significant for practical use of this effect.

3.2. EBSD Analysis of Microstructure

Figure 2 shows the EBSD maps of grain orientations, spectra of grain misorientation angles, and gran size distributions in the alloy after equal-channel angular pressing and further annealing at 370°C. As can

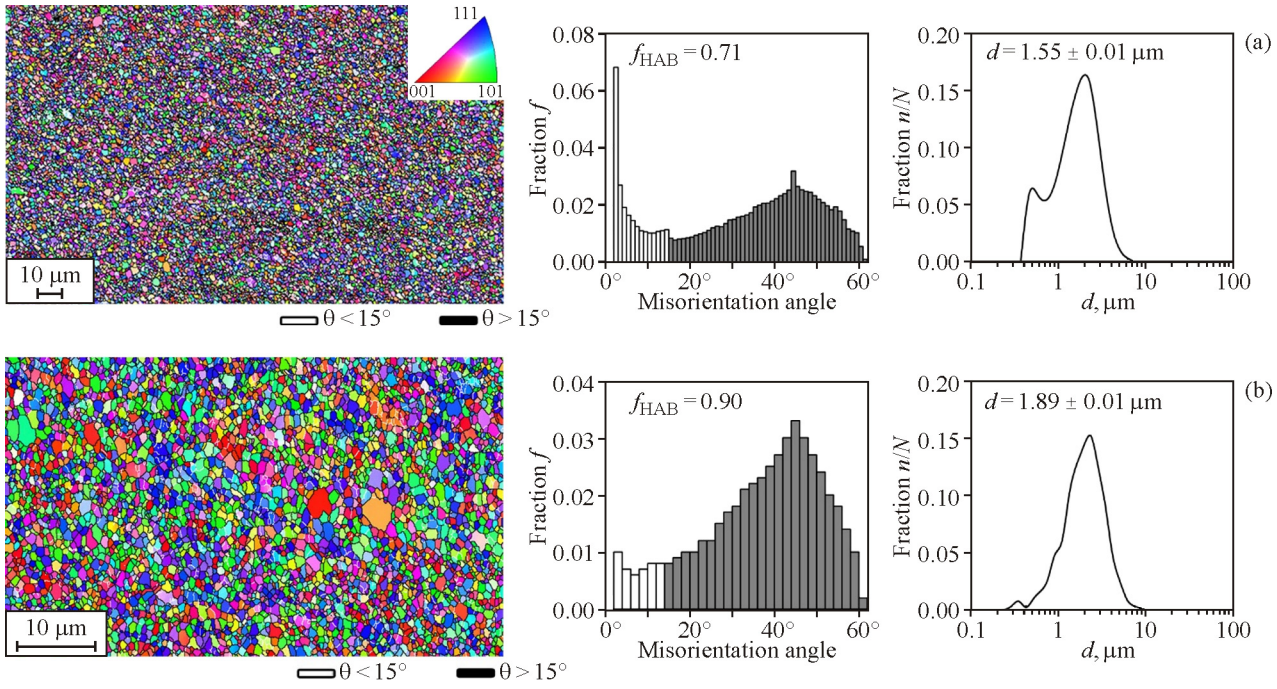

Fig. 2. Grain orientation maps, grain misorientation spectra, and grain size distributions in aluminum alloy 1420 after equal-channel angular pressing (a) and further annealing at 370°C (b), with orientation maps colored according to crystallographic orientation to normal and with low- and high-angle boundaries (HAB) colored respectively white and black (color online).

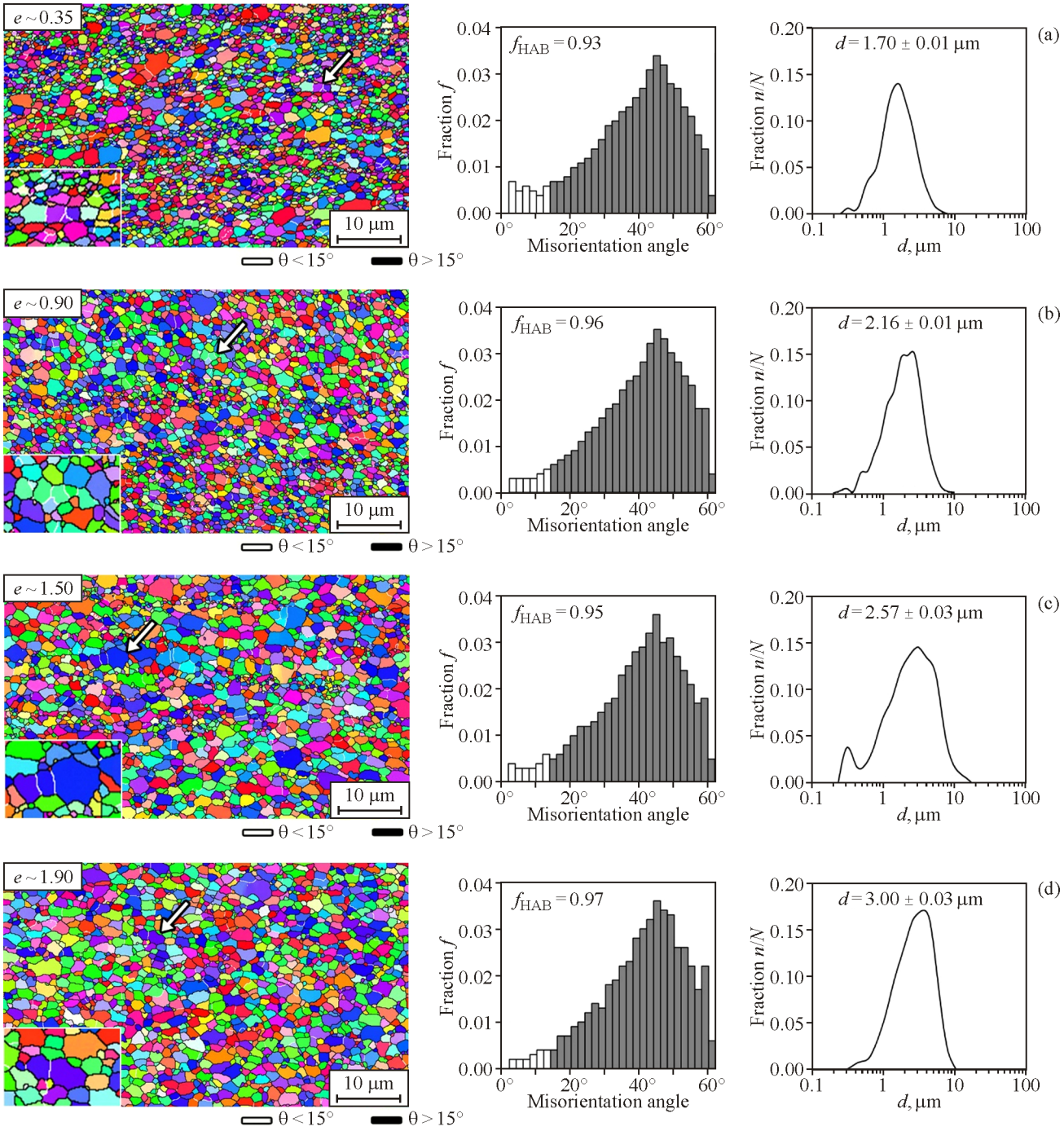

Fig. 3. Grain orientations maps, grain misorientation spectra, and grain size distributions in aluminum alloy 1420 deformed by tension to 35 (a), 150 (b), 350 (c), and 580% (d) in horizontal direction (color online).

be seen, the use of equal-channel angular pressing provides a structure with an average equiaxed grain size of about 1.6 μm, fraction of high-angle boundaries of 71% (Fig. 2b), and bimodal grain size distribution. Such a fine recrystallized structure is a necessary condition for the effect of superplasticity.

The fine structure formed by equal-channel angular pressing is not stable, and an increase in the grain size is observed even at the initial stages of further superplastic deformation. To distinguish between the influence of heating to the strain temperature and the influence of further deformation at the test tempera-

ture on the growth of grains, we analyzed the structure of a reference specimen after heating to 370°C and aging for 8 min under the same conditions without deformation. After such heat treatment, the average size of grains in the reference specimen increased to 1.9 μm (by 20%) while their shape remained equiaxed, the bimodal grain size distribution almost disappeared, and the fraction of high-angle boundaries increased to 90% (Fig. 2b). Obviously, such changes on heating without deformation are due to collective recrystallization in the reference specimen.

For analyzing the evolution of the microstructure under superplastic deformation, the specimens were tested for tension with different strain degrees under identical temperature-rate conditions. Four points marked as circles on the stress–strain curves in Fig. 1 were chosen for the analysis:

– strain ~35% (engineering curve peak, $e \sim 0.35$),
– strain ~150% (true curve peak, $e \sim 0.9$),
– strain ~350% (bend of both curves, $e \sim 1.5$),
– strain ~580% (bend of both curves, $e \sim 1.9$).

Figure 3 presents the results of our microstructural analysis at the middle of the specimen gage sections after deformation to the above strain degrees.

The analysis suggests that the deformation is accompanied by dynamic grain growth, with the average grain size reaching 3 μm at 580% and with the fraction of high-angle boundaries remaining almost constant and measuring 93–97%. The respective distributions of misorientation angles are close to random. Another feature is that the form of grains becomes clearly elongated in the direction of tension. Such elongated grains often reveal low-angle boundaries oriented across the direction of tension, which can readily be seen in the lower left corner of the orientation maps (insets). Bimodality is noticeable in the grain size distribution, suggesting the presence of finer grains. On the orientation maps, such fine grains are normally grouped into chains (Fig. 3, arrows) which are extended mainly in the direction of tension and the orientation of which is most often close to crystallographic (close colors on the maps); however, in some cases, high-angle misorientations are found in adjacent fine grains. These observations suggest that such a near-equiaxed structure can result from transverse separation of elongated grains, i.e., from continuous dynamic recrystallization through which new grains appear [23, 24]. It should be noted that continuous dynamic recrystallization during superplastic deformation is also observed in other materials, e.g., in Fe-based hard magnetic alloys [25].

Our additional EBSD analysis shows that crystallographic texture of the type $\{hkl\}\langle 100\rangle$ and $\{hkl\}\langle 111\rangle$ is formed during superplastic deformation. The texture of deformation arises only against the background of multiple dislocation glide along certain crystallographic planes. Any rare events of dislocation motion cannot lead to texture formation. The above observations and conclusions indicate that extensive intragranular glide occurs, as happens in other materials during superplastic deformation [15–23].

One of the factors evidencing the action of intragranular glide is the presence of dislocations in the volume of grains and at their boundaries. Here it should be noted that the idea of dislocation glide as one of the main mechanisms of superplastic deformation is not always confirmed by thin-foil transmission electron microscopy of classical superplastic materials. The explanation of the absence of dislocations is that they fail to form stable configurations due to small grain sizes, i.e., to the proximity of high-angle boundaries, and easily move to the boundaries of grains and are absorbed by them.

In our case, alloy 1420 contains uniformly distributed fine second phase particles (Al_2LiMg Al_3Li). The interaction of dispersoids of these phases with dislocations and water quenching of the specimens after deformation allowed us to identify their dislocation structure despite the small grain size. Figure 4 presents the results of thin-foil transmission microscopy: the microstructure of the reference specimen, which evidences the absence of dislocations before superplastic deformation, and the microstructure of the specimens deformed by tension to 150 and 580% ($e = 0.9$ and 1.9). After elongation by 150 and 580%, the dislocation density almost in all grains is high. As a large number of dislocations move in the volume of grains, the grains become markedly elongated (Figs. 4b, 4c). Such intergranular glide also results in dislocation pileups and in low-angle boundaries in individual elongated grains (Fig. 4c, arrow).

As a whole, the results of thin-foil transmission electron microscopy correlate with the results of our quantitative EBSD analysis. The bimodal grain size distribution identified by the EBSD method is likely due to the fragmentation of grains elongated during deformation through the formation of dislocation walls and low-angle boundaries across the deformation direction, and this provides the formation of fine equiaxed grains. The fragmentation of elongated grains is a continuous process successively covering

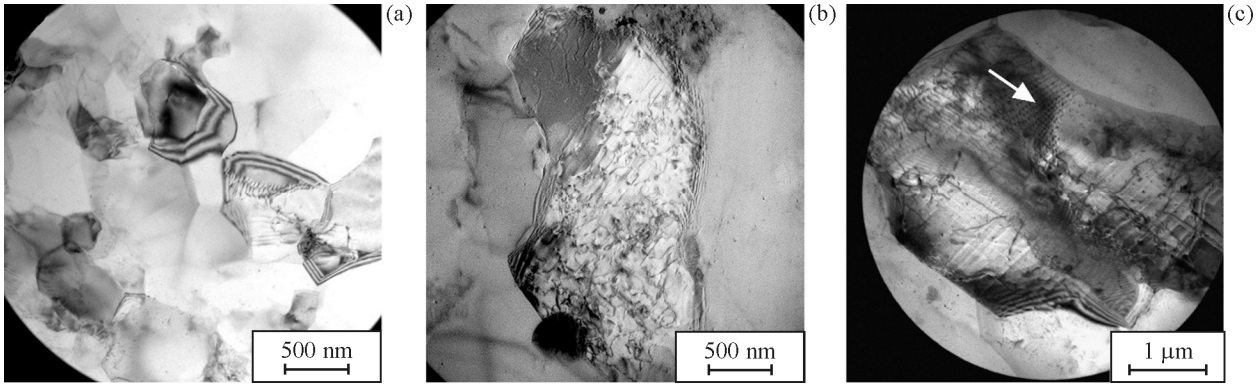

Fig. 4. Microstructure of aluminum alloy 1420 before (a) and after deformation to $e = 0.9$ (b) and 1.9 (c).

different specimen regions. Therefore, at all strain degrees, the grain size distribution is bimodal, and such bimodality is most pronounced at the initial stages of deformation.

4. DISCUSSION

From our mechanical tests in the mode of superplastic flow and microstructural analysis it follows that the material during its superplastic deformation experiences pronounced hardening (Fig. 1), grain growth and elongation (Fig. 3), intragranular substructure formation (Fig. 4), and crystallographic texture formation. According to the classical concepts, the main mechanism of superplasticity is grain boundary sliding, and the contribution of intragranular dislocation glide depends on the grain size [26]. Under the optimum temperature-rate conditions of superplasticity, the contribution of intragranular dislocation glide in rather coarse materials (average grain size ≥10 μm) can reach 1/5–1/4 while its contribution in fine materials (average grain size ~1.2 μm) is close to zero [26]. The explanation is that increasing the grain size decreases the diffusion mass transfer and increases the flow stress, and this provides the generation of a large number of lattice dislocations; that is, grain boundary sliding in coarse materials normally leads to stress concentration at triple junctions, and intragranular glide serves to accommodate these stresses [2]. The internal grain substructure observed in our study (Fig. 4) can be due to such accommodation glide. However, if the dominant process of superplastic flow was gran boundary sliding, any orientation relations between adjacent grains would be broken by grain displacements and rotations and no texture would be formed. On the contrary, the effect of active intragranular dislocation glide causes not only grain elongation but also texture formation, which is what we observed in our study.

Increasing the strain rate also impedes the diffusion and facilitates the generation of lattice dislocations, but the rate sensitivity thereby drops. In our case, at a strain rate of about 10^{-2} s^{-1}, the rate sensitivity is close to maximal: $m \approx 0.5$. Therefore, this rate corresponds to the optimum temperature-rate conditions of superplasticity, which agrees with the well-known fact that fine-grained materials, as a rule, show high-rate and/or low-temperature superplasticity. By estimates [20], the contribution of grain elongation to the total elongation of fine-grained alloy 1420 deformed under the same temperature-rate conditions can be rather high (~360% of ~1000%), and this also confirms the fact that the total strain is greatly contributed by intragranular glide.

Besides, the peak observed on the curve of superplastic flow is slightly diffused (Fig. 1b), which is associated with dynamic recrystallization. First, necessary critical strains are accumulated via multiple dislocation glide, and after approaching a sufficient dislocation density, continuous dynamic recrystallization with the formation of new grains begins. The driving force of such structural transformation is new dislocation pileups continuously generated via multiple dislocation glide. At the same time, the diffuse peak can be also an artifact associated both with diffuse necking and with variations in the rate sensitivity during deformation (in particular, due to dynamic grain growth).

5. CONCLUSION

Our analysis by transmission electron microscopy and electron backscatter diffraction allows the following conclusions on the behavior of Al-Mg-Li

with a uniform fine recrystallized microstructure at $T = 370°C$, $\dot{\varepsilon} = 3 \times 10^{-2}\ s^{-1}$, which corresponds to the temperature-rate conditions of superplastic flow for this alloy.

The structure of the alloy under deformation evolves mainly via dynamic grain growth and continuous dynamic recrystallization.

The effect of continuous dynamic recrystallization consists in transverse separation of elongated grains and further transformation into chains of almost equiaxed grains.

The fact of noticeable grain elongation, pronounced substructure formation, and crystallographic texture formation suggests that the deformation of the alloy under the given conditions of superplasticity is greatly contributed by intragranular glide.

FUNDING

The work was supported by RFBR grant No. 20-02-00331 (microstructural research and analysis of deformation mechanisms) and State Assignment for IMSP RAS (materials obtained by deformation methods). The equipment was provided by the Collaborative Access Center of IMSP RAS. The work by E.A. Korznikova was supported by the Ministry of Education and Science of the Russian Federation (State Assignment for USATU under agreement No. 075-03-2021-014/4).

REFERENCES

1. Bate, P.S., Ridley, N., and Zhang, B., Mechanical Behavior and Microstructural Evolution in Superplastic Al-Li-Mg-Cu-Zr AA8090, *Acta Mater*., 2007, vol. 55, pp. 4995–5006. https://doi.org/10.1016/j.actamat.2007.05.017
2. *Superplasticity and Grain Boundaries in Ultrafine-Grained Materials*, Zhilyaev, A.P., Pshenichnyuk, A.I., Utyashev, F.Z., and Raab, G.I., Eds., Woodhead Publishing, 2021, pp. 301–316. https://doi.org/10.1016/B978-0-12-819063-0.00004-7
3. Sitdikov, O., Avtokratova, E., and Markushev, M., Structure, Strength and Superplasticity of Ultrafine-Grained 1570C Aluminum Alloy Subjected to Different Thermomechanical Processing Routes Based on Severe Plastic Deformation, *Trans. Nonferrous Met. Soc. China*, 2021, vol. 31, pp. 887–900. https://doi.org/10.1016/S1003-6326(21)65547-4
4. Liu, F.C., Xue, P., and Ma, Z.Y., Microstructural Evolution in Recrystallized and Unrecrystallized Al–Mg–Sc Alloys during Superplastic Deformation, *Mater. Sci. Eng. A*, 2012, vol. 547, pp. 55–63. https://doi.org/10.1016/j.msea.2012.03.076
5. Kaibyshev, R., Goloborodko, A., Musin, F., Nikulin, I., and Sakai, T., The Role of Grain Boundary Sliding in Microstructural Evolution during Superplastic Deformation of a 7055 Aluminum Alloy, *Mater. Trans*., 2002, vol. 43, pp. 2408–2414. https://doi.org/10.2320/matertrans.432408
6. Xun, Y., Tan, M.J., and Nieh, T.G., Grain Boundary Characterisation in Superplastic Deformation of Al-Li Alloy Using Electron Backscatter Diffraction, *Mater. Sci. Tech*., 2004, vol. 20, pp. 173–180. https://doi.org/10.1179/174328413X13789824293786
7. Liu, Z., Li, P., Xiong, L., Liu, T., and He, L., High-Temperature Tensile Deformation Behavior and Microstructure Evolution of Ti55 Titanium Alloy, *Mater. Sci. Eng. A*, 2017, vol. 680, pp. 259–269. https://doi.org/10.1016/j.msea.2016.10.095
8. Li, J., Ren, X., and Gao, X., Effect of Superplastic Deformation on Microstructure Evolution of 3207 Duplex Stainless Steel, *Mater. Charact*., 2020, vol. 64, p. 110320. https://doi.org/10.1016/j.matchar.2020.110320
9. Lin, D., Hu, J., and Jiang, D., Superplasticity of Ni-Rich Single Phase NiAl Intermetallics with Large Grains, *Intermetallics*, 2005, vol. 13, pp. 343–349. https://doi.org/10.1016/j.intermet.2004.07.008
10. Jiang, D. and Lin, D., The Microstructural Evolution in Large-Grained Ni–40Al during Superplastic Deformation, *J. Alloy. Compd*., 2006, vol. 415, pp. 177–181. https://doi.org/10.1016/j.jallcom.2005.08.013
11. Niu, H.Z., Kong, F.T., Chen, Y.Y., and Zhang, C.J., Low-Temperature Superplasticity of Forged Ti–43Al–4Nb–2Mo–0.5B Alloy, *J. Alloy. Compd*., 2012, vol. 543, pp. 19–25. https://doi.org/10.1016/j.jallcom.2012.07.127
12. Johnson, R.H., Packer, C.M., Anderson, L., and Sherby, O.D., Microstructure of Superplastic Alloys, *Philos. Mag*., 1968, vol. 156, pp. 1309–1314.
13. Likhachev, V.A., Myshlayyev, M.B., Sen'kov, O.N., and Belyayev, S.P., Creep of Aluminum in Torsion under Superplastic Conditions, *Phys. Metal. Metallogr*., 1981, vol. 52, pp. 156–164.
14. Edington, J.W., Microstructural Aspects of Superplasticity, *Met. Trans. A*, 1982, vol. 13, pp. 703–715.
15. Perez-Prado, M.T., Cristina, M.C., Ruano, O.A., and Gonzalez-Doncel, G., Grain Boundary Sliding and Crystallographic Slip during Superplasticity of Al–5% Ca–5% Zn as Studied by Texture Analysis, *Mater. Sci. Eng. A*, 1998, vol. 244, pp. 216–223.
16. Mikhaylovskaya, A.V., Yakovtseva, O.A., Golovin, I.S., Pozdniakov, A.V., and Portnoy, V.K., Superplastic Deformation Mechanisms in Fine-Grained Al–Mg Based Alloys, *Mater. Sci. Eng. A*, 2015, vol. 627, pp. 31–41. https://doi.org/10.1016/j.msea.2014.12.099
17. Kanazawa, T., Masuda, H., Tobe, H., Kakehi, K., and Sato, E., Initial Process of Continuous Dynamic Recrystallization in a Superplastic Al-Mg-Mn Alloy, *J.*

Jap. Inst. Light Met., 2017, vol. 67, pp. 95–100. https://doi.org/10.2464/jilm.67.95

18. Myshlyaev, M., Mironov, S., Korznikova, G., Konkova, T., Korznikova, E., Aletdinov, A., and Khalikova, G., EBSD Study of Superplastically Strained Al-Mg-Li Alloy, *Mater. Lett*., 2020, vol. 275, p. 128063. https://doi.org/10.1016/j.matlet.2020.128063
19. Myshlyaev, M.M., Prokunin, M.A., and Shpeizman, V.V., Mechanical Behavior of Microcrystalline Aluminum-Lithium Alloy under Superplasticity Conditions, *Phys. Solid State*, 2001, vol. 43, pp. 865–870. https://doi.org/10.1134/1.1371367
20. Myshlyaev, M., Mironov, S., Korznikova, G., Konkova, T., Korznikova, E., Aletdinov, A., Khalikova, G., Raab, G., and Semiatin, S.L., EBSD Study of Superplasticity: New Insight into a Well-Known Phenomenon, *J. Alloy. Compnd*, 2021. https://doi.org/10.1016/j.jallcom.2021.162949
21. Myshlyaev, M.M., Speizman, V.V., Klubovich, V.V., Kulak, M.M., and Lyu, G., Change in Characteristics of Superplastic Deformation of the Aluminum-Lithium Alloy under the Effect of Ultrasonic Vibrations, *Phys. Sol. State*, 2015, vol. 57, pp. 2039–2044. https://doi.org/10.1134/S1063783415100236
22. Shakesheff, A.J. and Partridge, P.G., Superplastic Deformation of Al-Li-Cu Alloy Sheet, *J. Mater. Sci*., 1986, vol. 21, pp. 1368–1376.
23. Lin, D., Lin, T.L., Shan, A., and Chen, M., Superplasticity in Large-Grained Fe_3Al Alloys, *Intermetallics*, 1996, vol. 4, pp. 489–496.
24. Humphreys, F.J., Prangnell, P.B., Bowen, J.R., Gholinia, A., and Harris, C., Developing Stable Fine-Grained Microstructures by Large Deformation, *Philos. Trans. R. Soc. Lond. A*, 1999, vol. 357, pp. 1663–1681.
25. Korznikova, G.F., Structure Formation under Hot Compression Deformation of Hard Magnetic Alloy Fe–30%Cr–8%Co, *Fiz. Mezomekh*., 2015, vol. 18, no. 2, pp. 89–94. https://doi.org/10.24411/1683-805X-2015-00047
26. Novikov, I.I. and Portnoy, V.K., *Superplasticity of Ultrafine-Grained Alloys*, Moscow: Metallurgia, 1981.